Journal of Advanced Research 28 (2021) 255–267

Contents lists available at ScienceDirect

Journal of Advanced Research

journal homepage: www.elsevier.com/locate/jare

Quercitrin alleviates cartilage extracellular matrix degradation and delays ACLT rat osteoarthritis development: An in vivo and in vitro study

Hanli Guo [a,1], Weifeng Yin [b,1], Ziling Zou [a], Chao Zhang [a], Minghui Sun [c], Lingtian Min [c], Lei Yang [a,*], Lingyi Kong [a,*]

[a] Jiangsu Key Laboratory of Bioactive Natural Product Research and State Key Laboratory of Natural Medicines, School of Traditional Chinese Pharmacy, China Pharmaceutical University, Nanjing 210009, China
[b] Department of Orthopedics, Tongji Hospital, Tongji Medical College, Huazhong University of Science and Technology, Wuhan 430030, China
[c] Department of Joint Surgery, The Affiliated Drum Tower Hospital of Nanjing University Medical School, Nanjing 210009, China

HIGHLIGHTS

- The p110α protein levels were reduced in articular cartilage of ACLT rats.
- Quercitrin prominently alleviated tibial subchondral bone loss in ACLT rats.
- The p110α mRNA levels were dramatically downregulated in human OA cartilage.
- We first reported the effect of quercitrin on OA in vivo and vitro.
- Quercitrin exerts anti-OA effect by delaying ECM degradation.

GRAPHICAL ABSTRACT

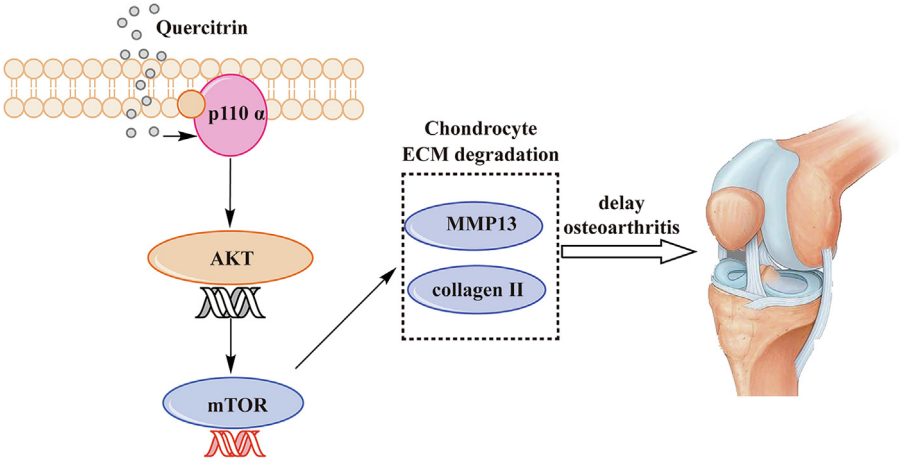

ARTICLE INFO

Article history:
Received 11 March 2020
Revised 1 June 2020
Accepted 22 June 2020
Available online 24 June 2020

Keywords:
Osteoarthritis
Quercitrin
Phosphatidylinositol 3-kinase p110α

ABSTRACT

Introduction: Disruptions of extracellular matrix (ECM) degradation homeostasis play a significant role in the pathogenesis of osteoarthritis (OA). Matrix metalloproteinase 13 (MMP13) and collagen Ⅱ are important components of ECM. Earlier we found that quercitrin could significantly decrease MMP13 gene expression and increase collagen Ⅱ gene expression in IL-1β -induced rat chondrocytes and human chondrosarcoma (SW1353) cells.
Objectives: The effects and mechanism of quercitrin on OA were explored.
Methods: Molecular mechanisms of quercitrin on OA were studied in vitro in primary chondrocytes and SW1353 cells. An anterior cruciate ligament transection (ACLT) rat model of OA was used to investigate the effect of quercitrin in vivo. Micro-CT analysis and Safranin O-Fast Green Staining of knee joint

Abbreviations: OA, osteoarthritis; MMP13, matrix metalloproteinase 13; ECM, extracellular matrix; ACLT, anterior cruciate ligament transection; DMOAD, disease-modifying OA drug; BV/TV, bone volume/tissue volume; OARSI, Osteoarthritis Research Society International; NSAIDs, non-steroidal anti-inflammatory drugs; PI3K, Phosphatidylinositol 3-kinase; p110α, Phosphatidylinositol 3-kinase p110α.

Peer review under responsibility of Cairo University.

* Corresponding authors.
E-mail addresses: dorothy19802003@gmail.com (L. Yang), cpu_lykong@126.com (L. Kong).

[1] These authors contributed equally to this work.

https://doi.org/10.1016/j.jare.2020.06.020
2090-1232/

Extracellular matrix degradation
MMP13

samples were performed to observe the damage degree of tibial subchondral bone. Immunohistochemistry of knee joint samples were conducted to observe the protein level of MMP13, collagen Ⅱ and p110α in articular cartilage.

Results: In vitro, quercitrin promoted cell proliferation and delayed ECM degradation by regulating MMP13 and collagen II gene and protein expressions. Moreover, quercitrin activated the Phosphatidylinositol 3-kinase p110α (p110α)/AKT/mTOR signaling pathway by targeting p110α. We also firstly showed that the gene expression level of p110α was remarkably decreased in cartilage of OA patients. The results showed that intra-articular injection of quercitrin increased bone volume/tissue volume of tibial subchondral bone and cartilage thickness and reduced the Osteoarthritis Research Society International scores in OA rats. Meanwhile, immunohistochemical results showed that quercitrin exerted anti-OA effect by delaying ECM degradation.

Conclusion: These findings suggested that quercitrin may be a prospective disease-modifying OA drug for prevention and treatment of early stage OA.

Introduction

Osteoarthritis (OA) is a universal epidemic and age-related progressive joint disorder characterized by articular cartilage degeneration, osteophyte formation and functional impairment [1–4]. As life expectancy increases, OA has gradually become one of the most widespread chronic illnesses, resulting in physical disabilities and a reduced quality of life among the elderly population [5]. To date, the current treatment of OA is focused on pain relief, including the use of oral nonsteroidal anti-inflammatory drugs (NSAIDs) and intra-articular injections of hyaluronic acid and steroids. In the late stage of the disease, the present treatment strategy is joint replacement surgery [6–9]. Therefore, there is currently no effective disease-modifying therapy for OA, and identifying a disease-modifying OA drug (DMOAD) is urgently needed to alleviate and reverse the development of OA [10].

Degradation of the cartilage extracellular matrix (ECM) is considered as a OA hallmark and degradation of the cartilage ECM could be an underlying mechanism [10]. As the only unique organized cells in articular cartilage, chondrocytes synthesize dense ECM components that primarily include aggrecan and collagen II and play a pivotal part in maintaining cartilage homeostasis via an equilibrium between ECM catabolism and anabolism [11,12]. The basic feature of OA is the repression of aggrecan and collagen II expression [13,14], while the expression of matrix-degenerating enzymes such as matrix metalloproteinase13 (MMP13) is increased [15]. MMP13 is an enzyme mainly responsible for ECM degradation [16,17]; MMP-13 can hydrolyze collagen Ⅱ, the primary protein in the cartilage ECM [18,19]. Emerging evidence has shown that MMP13, which plays a vital part in OA progression, is considered a significant biomarker to assess OA therapeutic effects and OA progression [20–22]. Many studies have shown that aberrantly expressed genes in OA articular chondrocytes are one of its causes [23]. Therefore, inhibiting MMP13 expression and promoting collagen II accumulation in cartilage would be effective to relieve OA.

MMP13 overexpression is regulated by complicated signals in the PI3K/AKT/mTOR pathway [24,25], which is activated in many different cancers [26]. PI3Ks regulate cancer markers, such as those for cell survival, proliferation, migration, protein synthesis, glucose homeostasis and genomic instability [27,28]. There are four types of PI3Ks: type I, II and III are lipid kinases, and type IV is a Ser/Thr protein kinase [29,30]. Type IA PI3Ks (PI3Kα, PI3Kβ, and PI3Kδ) are heterodimers containing the Phosphatidylinositol 3-kinase p110 (p110) catalytic subunit (Phosphatidylinositol 3-kinase p110α(p110α), p110β, and p110δ) and a regulatory subunit [31]. PI3K activation is currently caused by mutations in the p110α subunit, which is called *PIK3CA* in many cancers [32], and p110α is a promising drug target for cancer chemotherapy [27].

Previous studies have indicated that the Phosphatidylinositol 3-kinase(PI3K)/AKT/mTOR signaling pathway plays a crucial part in the pathogenesis of OA [25,33–36]. Increasing evidence suggests that PI3K is closely related to OA. ChenCai et al. [25] proved that PI3K mRNA levels were downregulated in IL-1β-induced articular chondrocytes and human OA cartilage, which is different from normal cells and tissues. However, the role of p110α in OA remains unknown.

Parasitic loranthus (*Taxillussutchuenensis* (DC.) Danser), a traditional herbal medicine, has a long history of being used for the treatment and prevention of OA in China [37–39].

Quercitrin is a yellow-colored flavonoid and an important component among the total flavonoids in *Taxillussutchuenensis* (DC.) Danser [40]. The chemical structure of quercitrin is shown in Fig. 1A. To date, numerous studies have indicated that quercitrin has a series of biological activities including antioxidation [41,42], anti-inflammation [43,44], and neuropharmacological actions [45]. Pharmacological study has also confirmed that quercitrin could enhance osteoblast differentiation and inhibit osteoclast formation [46], reverse dysfunction induced by oxidative stress [47], and attenuate osteoporosis [48]. These findings have revealed that quercitrin is effective for the treatment of bone-related disorders. Accordingly, we explored whether quercitrin has therapeutic effects for OA.

In this paper, the effects of quercitrin on gene and protein expression of MMP13 and collagen Ⅱ in rat primary chondrocytes and human chondrosarcoma cells (SW1353) were explored. We further explored the mechanism of quercitrin associated the degradation delay of ECM in vitro and evaluated p110α mRNA levels in human OA and healthy articular cartilage. To further confirm the effect of quercitrin against OA in vivo, micro-CT analysis and Safranin O-Fast Green Staining of knee joint samples were performed to observe the damage degree of tibial subchondral bone. Immunohistochemistry of knee joint samples were conducted to observe the protein level of MMP13, collagen Ⅱ and p110α in articular cartilage.

Materials and methods

Materials

Quercitrin (quercetin 3-rhamnoside, PubChem CID: 5280459) (Q109798, Aladdin, China) was dissolved in dimethyl sulfoxide for cell treatment and was dissolved in 40% PEG400 for intra-articular injection in anterior cruciate ligament transection (ACLT) rats.

The materials used for this study included collagenase II (40508ES60, Yeasen, China); DMEM (SH30022.01B, HyClone, USA); fetal bovine serum (900–108, GeminiBio, USA); Nutrient mixture

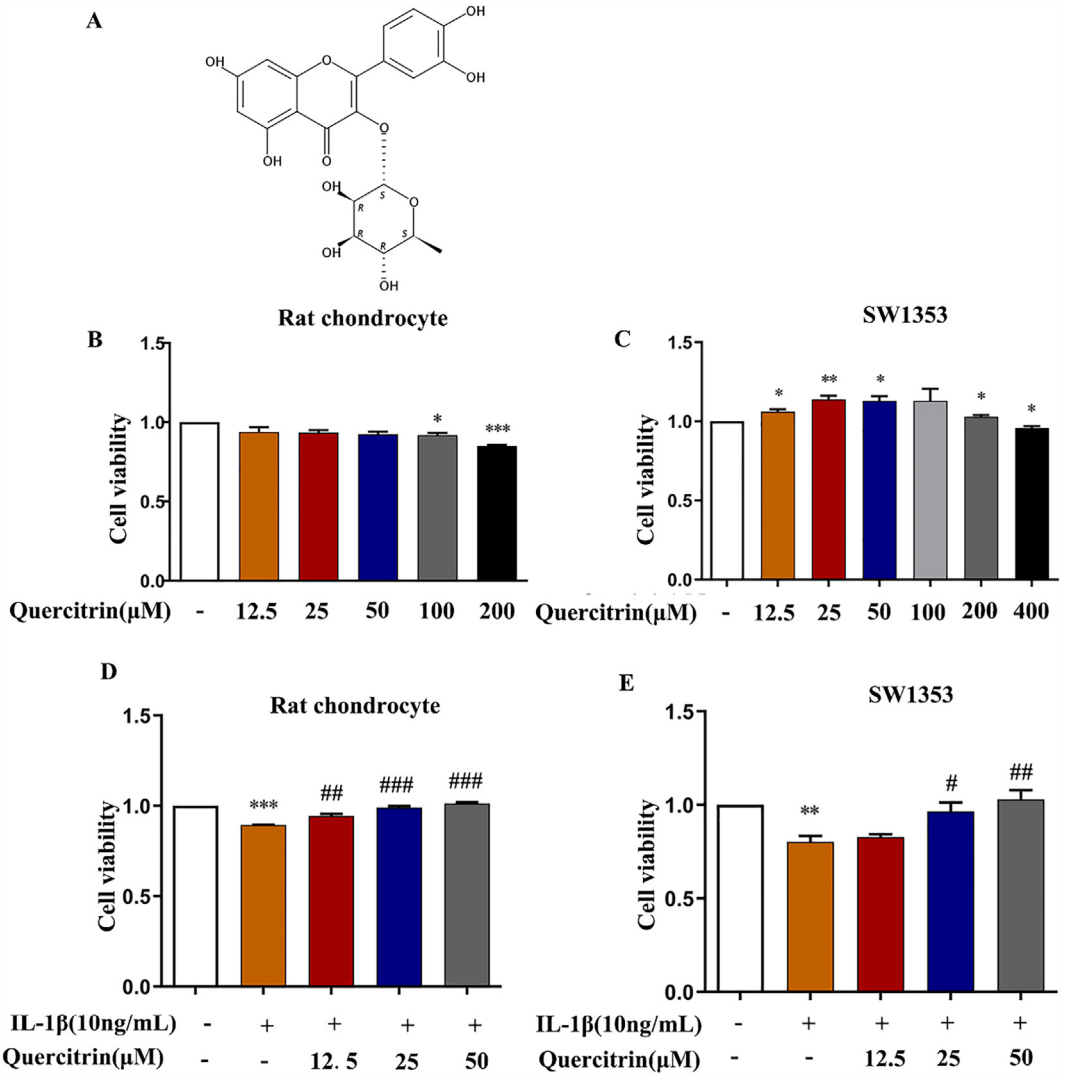

Fig. 1. The cytotoxic effects of quercitrin on chondrocytes. (A) Chemical structure of quercitrin $C_{21}H_{20}O_{11}$. (B–C) The cell viability of rat chondrocytes and SW1353 cells that were treated with different concentrations of quercitrin for 48 h as detected by CCK8 assay. (D-E) Rat chondrocytes and SW1353 cells were pretreated with IL-1β (10 ng/ml) for 2 h prior to treatment with different concentrations of quercitrin (12.5, 25, and 50 μM) for 48 h. The cell viability was measured by CCK8 assay. All experiments were repeated at least three times with similar results. All data are represented as the mean ± SD. Viability (CCK8) results were assessed by a one-way ANOVA, followed by Tukey's range test. *P < 0.05, **P < 0.01 and ***P < 0.001 versus the control group; #P < 0.05, ##P < 0.01 and ###P < 0.001 versus the IL-1β-treated group.

F-12 Ham (N3520, Sigma, USA); Cell Counting Kit-8 (C0038, Beyotime, China); and an RNA-Quick Purifications Kit (RN001, RN002, Yishan, China). We purchased recombinant rat IL-1β(400-01B, PeproTech, USA) and recombinant human IL-1β(200-01B, PeproTech, USA), as well as the following antibodies: anti-MMP13 (DF6494, 1:1000, Affinity, USA); anti-collagen Ⅱ (ab34712, 1:5000, Abcam, USA); anti-p-AKT (A5030, 1:500, Bimake, USA); and anti-GAPDH (200306-7E4, 1:10000, Zen BioScience, China). Anti-p110α (4249S, 1:1000), anti-p-mTOR (2971, 1:1000), anti-p85α (4292S, 1:1000,), anti-AKT (9272S, 1:1000) and anti-mTOR (2972, 1:1000) were purchased from Cell Signaling Technology.

Cell culture

The primary rat chondrocytes were isolated from SD rats as previously described [49]. Briefly, knee cartilage was harvested from 7-day-old SD rats and cartilage pieces were digested with 0.2% collagenase II and 0.25% trypsin for 30 min and 8–12 h, respectively. A 100-μm cell strainer was used to filter the cell suspensions, and the cells were cultured with DMEM containing 10% fetal bovine serum [50]. Human chondrosarcoma (SW1353) cells have a similar phenotype to chondrocytes and are often used for research on chondrocytes and related diseases [51]. SW1353 cells were purchased from the Cell Bank of Shanghai Institute of Biochemistry and Cell Biology and were cultured in F-12 containing 10% fetal bovine serum. Cells were pretreated with quercitrin for 2 h in advance and then induced with 10 ng/ml IL-1β for 48 h in the current and following experiments, barring special instructions.

Cell viability assay

The Cell Counting Kit-8 (CCK-8) assay was used to detect cell viability. Rat chondrocytes (4×10^3 cells/well) and SW1353 cells (3×10^3 cells/well) were seeded in 96-well plates. After 12 h of incubation, the cells were treated with various concentrations of quercitrin (0, 12.5, 25, 50, 100, and 200 μM) for 48 h, and cell viability was assessed using the CCK-8 assay as previously described [52,53].

Patient specimen selection

OA articular cartilage (n = 12) was obtained from patients who underwent knee replacement surgery. Normal articular cartilage

(n = 6) was collected from traumatic amputees without OA and rheumatoid arthritis and were used as controls. Informed consent forms were signed by all patients. Human ethical clearance of this experiment has been allowed by China Pharmaceutical University. All experimental procedures were approved by the Ethical Committee of China Pharmaceutical University. Ethical committee number for the study: CCPU 2019-084. Total RNA was extracted from OA articular cartilage and normal articular cartilage by RNA-Quick Purifications Kit (RN002, Yishan, China). The mRNA expression levels of p110α were assessed by RT-PCR.

Animals and experimental groups

Ethical committee number for the study: CCPU 2019-071. All animal experimental procedures were performed in accordance with protocols approved by the Institutional Animal Care and Use Committee (IACUC) of China Pharmaceutical University Experimental Animal Center. Male SD rats (200 ± 20 g) were obtained from Qinglongshan Animal Breeding Field (Nanjing, China). The SD rats were adapted for 1 week before surgery. Rats were randomly divided into the following four groups (n = 12 per group): sham-operated group, ACLT-induction, ACLT + quercitrin (2 mg/kg) and ACLT + quercitrin (4 mg/kg). The rats were anesthetized by intraperitoneally injection of 5% pentobarbital sodium and ACLT was performed on the right knee joint.

The rats were intraperitoneally injected with penicillin on the 1st to 3rd days after surgery to prevent infection. From the 4th day after the operation, different concentrations (10 mg/ml and 20 mg/ml) of quercitrin were injected into the right knee joints twice a week. The sham-operated group and ACLT-induction group received intra-articular injections of 50 μl of the vehicle used to dissolve quercitrin twice a week. Six rats were sacrificed at 4 and 8 weeks after the operation. Subsequently, the right knee joints were removed after sacrificing the rats and were immersed in 4% paraformaldehyde. These joints were scanned by Scanco viva CT 40 (SCANCO Medical AG, Switzerland) and were used for Safranin O-Fast Green Staining and immunohistochemistry.

Real-Time PCR

Total RNA was extracted from rat primary chondrocytes and SW1353 using the RNA-Quick Purification Kit (RN001, Yishan, China) according to the manufacturer's protocol. RNA was reverse-transcribed to complementary DNA (cDNA) using HiScript II Q RT SuperMix for qPCR (+gDNA wiper) (R223-01, Vazyme, China). Taq-Man polymerase with SYBR Green fluorescence was used for RT-PCR using a Light Cycler 480 Detector (Roche, Mannheim). The results were shown as a threshold cycle (Ct). The mRNA expression levels were quantified by glyceraldehyde 3-phosphate dehydrogenase (GAPDH) mRNA controls with the comparative $2^{-\Delta\Delta Ct}$ method. The primer sequences are shown in Table1.

Western blot

RIPA lysis buffer (P0013K, Beyotime, China) was used to lyse the cells, after which the lysate was centrifuged at 12,000 rpm for 15 min. Per a previous report, protein levels were measured using a BCA protein assay [54]. Protein sample was separated by 8–12% SDS-PAGE gel (60μg protein/lane) followed by the transference to polyvinylidene fluoride membranes (Millipore Corporation, MA, USA). These membranes were incubated at room temperature in blocking buffer (Tris buffer saline-Tween20 (TBST) containing of 5% skim milk) for 2 h and then incubated with the primary antibodies overnight at 4℃, followed by washed three times with TBST. Subsequently, these membranes were incubated with corresponding secondary antibodies for 2 h. ChemiDOCTM (Bio-RadLaboratories, Hercules, CA) was used to measure bound immuno-complexes. Image Lab 4.0 as used to assess the band intensity.

Table 1
Rat and Human primer sequences for RT-PCR.

Gene		Primer sequence (5′–3′)
GAPDH (Rat)	**F**	5′-TGGAGTCTACTGGCGTCTT-3′
	R	5′-TGTCATATTTCTCGTGGTTCA-3′
MMP13 (Rat)	**F**	5′-AGCTCCAAAGGCTACAACTTAT-3′
	R	5′-GTCTTCATCTCCTGGACCATAG-3′
Collagen Ⅱ (Rat)	**F**	5′-CACCGCTAACGTCCAGATGAC-3′
	R	5′-GGAAGGCGTGAGGTCTTCTGT-3′
GAPDH (Human)	**F**	5′-AGAAGGCTGGGGCTCATTT-3′
	R	5′-GGTGCTAAGCAGTTGGTGGT-3′
MMP13 (Human)	**F**	5′-ACTGAGAGGCTCCGAGAAATG-3′
	R	5′-GAACCCCGCATCTTGGCTT-3′
Collagen Ⅱ (Human)	**F**	5′-TGGACGATCAGGCGAAACC-3′
	R	5′-GCTGCGGATGCTCTCAATCT-3′
P110α (Human)	**F**	5′-CCACGACCATCATCAGGTGAA-3′
	R	5′-CCTCACGGAGGCATTCTAAAGT-3′

5-Ethynyl-2′-deoxyuridine (EdU) incorporation assay

The EdU labeling kit (C10310, Ribobio, China) was used to perform the EdU incorporation assay according to previously described methods [55]. The visualization of EdU was carried out with an ImageXpress® Micro system (Molecular Devices, CA). Red fluorescence was used to represent the cells that were undergoing cell replication during incubation.

Immunofluorescences

SW1353 cells were fixed 4% paraformaldehyde for 15 min, followed by incubated in 5% bovine serum albumin (BSA) containing 0.1% Triton X-100 for 60 min. Subsequently, the SW1353 cells were incubated with anti-collagen Ⅱ (ab34712, 1:200 dilution, Abcam) overnight at 4 °C. The secondary antibody was Alexa Fluor® 488 AffiniPure Goat Anti-Rabbit IgG (H + L) (33106ES60, Yeasen, China). The cell nuclei were stained with DAPI. The visualization of immunofluorescence experiments was carried out with an ImageXpress® Micro system (Molecular Devices, CA).

Small interfering RNA-mediated gene silencing

P110α small interfering RNAs (p110α siRNAs) (5′-GGU UAA AGA UCC AGA AGU ATT-3′ and 5′-UACUUCUGGAUCUUUAACCTT-3′)

Fig. 2. Quercitrin suppressed MMP13 expression and increased collagen Ⅱ deposition in IL-1β-induced rat chondrocytes and SW1353 cells. (A–D) Rat chondrocytes and SW1353 cells were pretreated with IL-1β (10 ng/ml) for 2 h prior to treatment with different concentrations of quercitrin (12.5, 25, and 50 μM) for 48 h. The cells were collected and collagen II and MMP13 mRNA expression levels were evaluated by RT-PCR. (E-J) Rat chondrocytes and SW1353 cells were pre-treated with IL-1β (10 ng/ml) for 2 h prior to treatment with different concentrations of quercitrin (12.5, 25, and 50 μM) for 48 h. The cells were collected and collagen II and MMP13 protein expression levels were evaluated by western blot. RT-PCR and western blot were repeated at least three times with similar results. All data are represented as the mean ± SD. *P < 0.05, **P < 0.01and ***P < 0.001 versus the control group; #P < 0.05, ##P < 0.01 and ###P < 0.001 versus the IL-1β-treated group. (K) Compared with control (n = 6), p110α mRNA expression levels were significantly decreased in severe OA patients (n = 12) by RT-PCR. ***P < 0.001 versus the control. Data from RT-PCR and western blot were analyzed by using one-way ANOVA, followed by Tukey's range test.

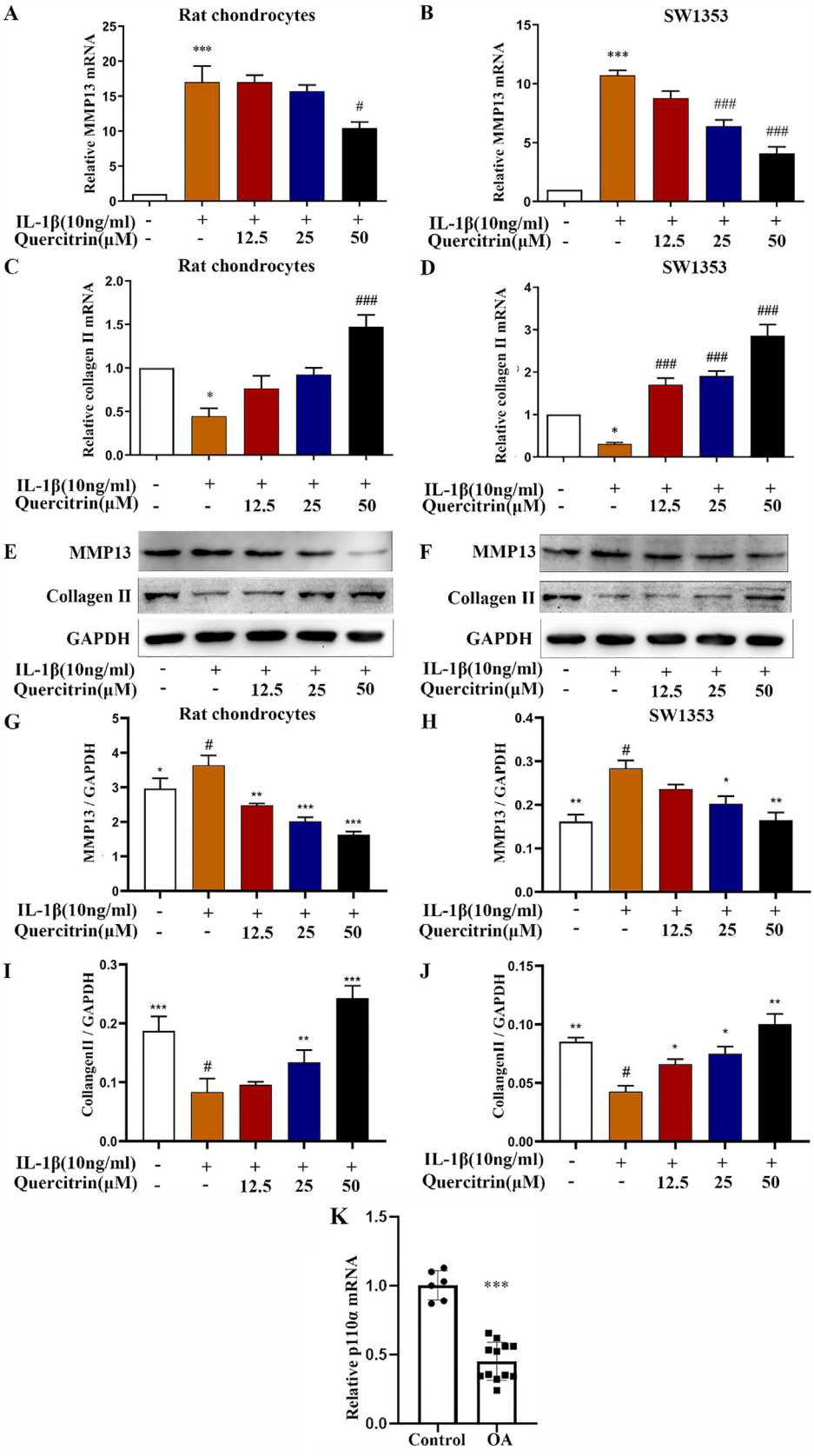
A
Rat chondrocytes
Relative MMP13 mRNA
IL-1β(10ng/ml)
Quercitrin(μM)
B
SW1353
C
Rat chondrocytes
Relative collagen II mRNA
D
SW1353
E
MMP13
Collagen II
GAPDH
F
G
Rat chondrocytes
MMP13 / GAPDH
H
SW1353
I
CollagenII / GAPDH
J
K
Relative p110α mRNA
Control
OA

and nontargeting small interfering RNAs (NC siRNAs) (5′-UUCUCC GAACGUGUCACGUTT-3′ and 5′-ACGUGACACGUUCGGAGAATT-3′) were synthesized by General Biosystems (Chuzhou, China). SW1353 cells (3×10^5cells/well) were seeded in six well plates. When cells growth reaches 70–75%, the siRNAs were transfected into SW1353 cells using the Lipofectamine 3000 (L3000008, Invitrogen, USA) according to the manufacturer's protocol. The NC siRNAs were transfected under the same conditions [56].

Micro-Computed Tomography (Micro-CT) analysis

Micro-CT was used to evaluate the tibial subchondral bone in the ACLT rat specimens. The subchondral bone density of tibiae was scanned using serial 21-μm tomographic images at 70 kV with a Scanco viva CT 40 (SCANCO Medical AG, Switzerland) according to a previous study [57]. Built-in software in the μ-CT system was used for three-dimensional reconstruction. Bone volume/tissue volume (BV/TV) of tibial subchondral bone was evaluated in the μ-CT system.

Immunohistochemistry

It has been noted, the right knee joints were removed after sacrificing the rats [58]. The right knee joints samples were immersed in 4% paraformaldehyde for two days, followed by decalcified in 10% EDTA Decalcifying solution (G1105, Servicebio, China) for 4 weeks and embedded in paraffin wax. Safranin O-Fast Green Staining and immunohistochemistry staining of MMP13, collagen Ⅱ and p110α were performed [59]. The severity of cartilage degeneration was examined with an Osteoarthritis Research Society International (OARSI) OA cartilage histopathology assessment system as previously described [60].

Statistical analysis

There are at least three times of vitro experiments with similar results. All of the data were analyzed with one-way, followed by Tukey's range test. All data are presented as the mean ± standard deviation (SD). *, **, *** indicate $p < 0.05$, 0.01 and 0.001. #, ##, ### indicate $p < 0.05$, 0.01 and 0.001.

Results

Effects of quercitrin on rat primary chondrocytes and SW1353 cells viability.

The underlying cytotoxicity of quercitrin on rat chondrocytes and SW1353 cells were assessed by CCK8 assay. The CCK8 assay showed that quercitrin displayed no cytotoxicity on rat chondrocytes or SW1353 cells at concentrations ranging from 0 to 50 μM (Fig. 1B and C). Therefore, we selected concentrations of 12.5, 25, and 50 μM for the subsequent experiments.

The effects of quercitrin on IL-1β-stimulated rat chondrocytes and SW1353 cells were assessed. The results demonstrated that quercitrin could significantly prevent the inhibitory effects of IL-1β stimulation on cell viability at concentrations of 12.5, 25, and 50 μM in a dose-dependent manner in rat chondrocytes and SW1353 cells (Fig. 1D and E).

Quercitrin suppressed MMP13 expression and increased collagen Ⅱ deposition in IL-1β-induced rat chondrocytes and SW1353 cells.

As we know, IL-1β plays a vital part in cartilage degradation by suppressing ECM synthesis [58]. Thus, we explored the effects of quercitrin on MMP13 and collagen Ⅱ expression in IL-1β-induced rat chondrocytes and SW1353 cells. The average value of MMP13 mRNA expression in IL-1β-induced was 17.00 ± 4.01, which was higher than control (1.00 ± 0.00) ($P < 0.001$) in rat chondrocytes (Fig. 2A). The average value of collagen Ⅱ mRNA expression in IL-1β-induced was 0.44 ± 0.16, which was lower than control ($P < 0.05$) in rat chondrocytes (Fig. 2C). The average value of MMP13 mRNA expression in IL-1β-induced was 10.72 ± 0.75, which was higher than control ($P < 0.001$) in SW1353 (Fig. 2B). The average value of collagen Ⅱ mRNA expression in IL-1β-induced was 0.30 ± 0.06, which was lower than control ($P < 0.05$) in SW1353 (Fig. 2D). The RT-PCR results showed that quercitrin markedly inhibited MMP13 gene expression and increased collagen Ⅱ gene expression in a dose-dependent manner (Fig. 2A–D). Western blot also indicated the same effects (Fig. 2E–J).

p110α mRNA levels were reduced in human OA articular cartilage

To investigate the involvement of p110α in the process of OA, RT-PCR experiments were used to assess p110α mRNA levels in human OA (n = 12) and healthy (n = 6) samples. The average value of p110α mRNA expression in human OA cartilage was 0.45 ± 0.14, which was lower than healthy samples (1.00 ± 0.11) ($P < 0.001$) (Fig. 2K). The RT-PCR results revealed that p110α mRNA expression was significantly decreased in human OA cartilage relative to healthy samples.

Quercitrin activated the p110α/AKT/mTOR signaling pathway by targeting p110α

The protein expression of p110α, p-AKT and p-mTOR was suppressed after stimulation with IL-1β, and quercitrin increased the expression of these proteins in a dose-dependent manner in rat chondrocytes and SW1353 cells (Fig. 3A–H). The transfection efficiency of p110α siRNAs in SW1353 cells was confirmed by RT-PCR (supplement Fig. 1A). We analyzed the effects of *PIK3CA* silencing on matrix biomarkers including collagen Ⅱ and MMP13. The protein expression of MMP13 was increased and collagen Ⅱ was decreased in the IL-1β-stimulated and *PIK3CA*-silenced groups, though these effects were reversed by quercitrin (Fig. 3I–K). The effects on collagen Ⅱ were further confirmed by immunofluorescence (Fig. 3L).

Next, we evaluated the effects *PIK3CA* silencing on rat chondrocytes proliferation. EdU staining experiments showed that the number of red proliferating cells is reduced in the IL-1β-stimulated and *PIK3CA*-silenced groups, and these effects were reversed by quercitrin (Fig. 3M). Collectively, these results revealed that *PIK3CA* silencing could suppress chondrocytes matrix synthesis and proliferation and that these effects were reversed by quercitrin.

Intra-articular injection of quercitrin delayed cartilage degeneration

To evaluate the effects of quercitrin on progression of OA histologically, intra-articular injections of quercitrin into ACLT rats was performed (Fig. 4A). Safranin O-Fast Green Staining was used to evaluate the loss of proteoglycans in keen cartilage. As shown in Fig. 4B, we observed markedly more damage to the articular cartilage and more severe proteoglycan loss in the ACLT rats at 8 weeks than at 4 weeks, which indicated that ACLT rats' knee joints exhibited more osteoarthritic changes at 8 weeks than at 4 weeks. At 4 and 8 weeks, intra-articular injection with quercitrin (2 mg/kg and 4 mg/kg) alleviated all cartilage damage and rescued the proteoglycan contents in the articular cartilage compared with ACLT rats.

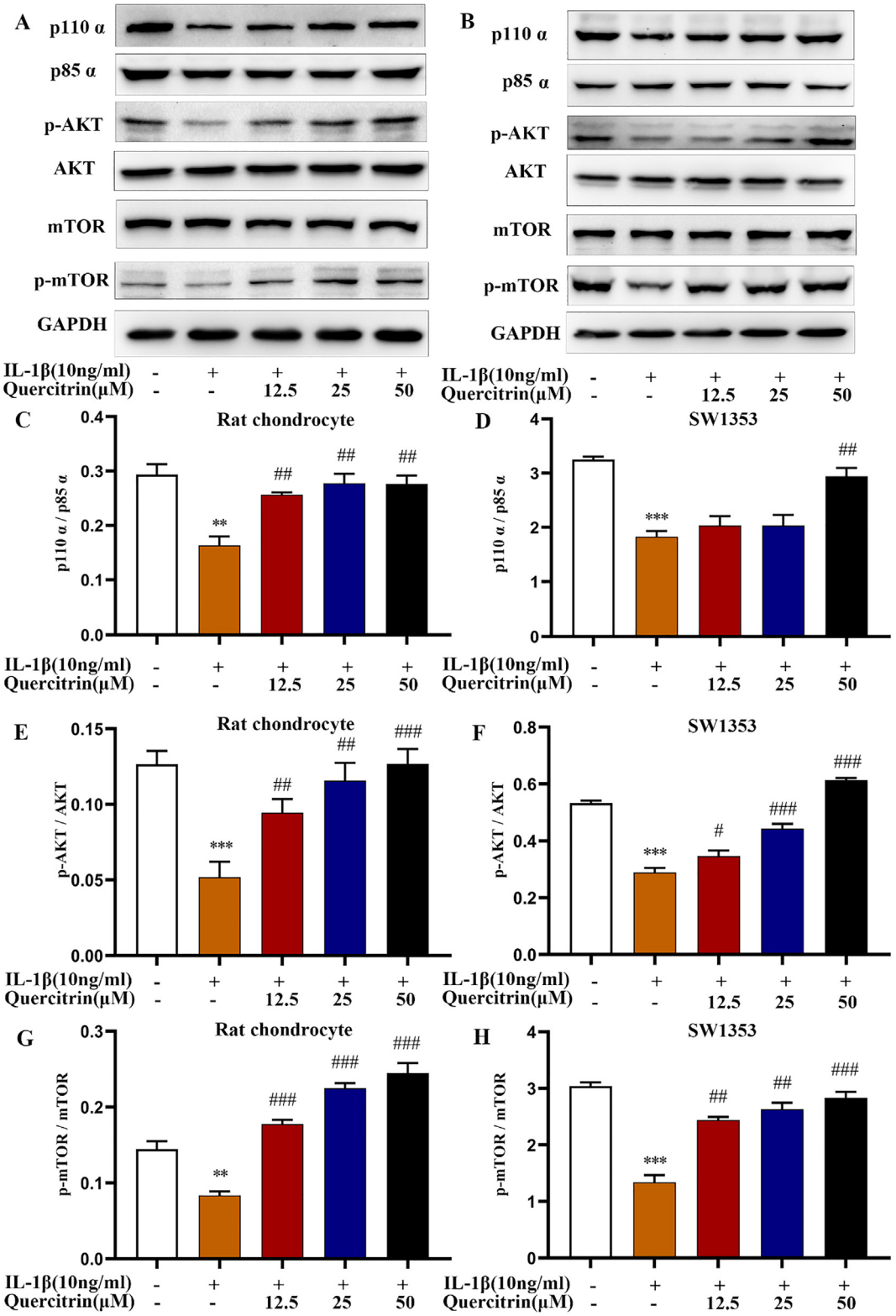

Fig. 3. Quercitrin activated the p110α/AKT/mTOR signaling pathway by targeting p110α. (A–H) Rat chondrocytes and SW1353 cells were pretreated with IL-1β (10 ng/ml) for 2 h prior to treatment with different concentrations of quercitrin (12.5, 25, and 50 μM) for 48 h. The p110α, p85α, p-AKT, t-AKT, p-mTOR, and t-mTOR protein expression levels were evaluated by western blot. All data are represented as mean ± SD. *P < 0.05, **P < 0.01 and ***P < 0.001 versus the control group; #P < 0.05, ##P < 0.01 and ###P < 0.001 versus the IL-1β treated group. (I-K) NC and p110α siRNAs transfected into SW1353 cells. Twelve hours after transfection, the cells were IL-1β and quercitrin for 48 h, after which the cells were used for the following experiments. MMP13 and collagen Ⅱ protein expression were evaluated by western blot. All data are represented as the mean ± SD. ***P < 0.001 versus the control group; #P < 0.05 and ##P < 0.01 versus the IL-1β treated group; &P < 0.05 versus the IL-1β and quercitrin treated group. (L) Collagen Ⅱ was evaluated by immunofluorescence. (M) EdU staining experiments are used to observe red proliferating cells. All experiments were repeated at least three times with similar results. Data from RT-PCR and western blot were analyzed by using one-way ANOVA, followed by Tukey's range test. (For interpretation of the references to colour in this figure legend, the reader is referred to the web version of this article.)

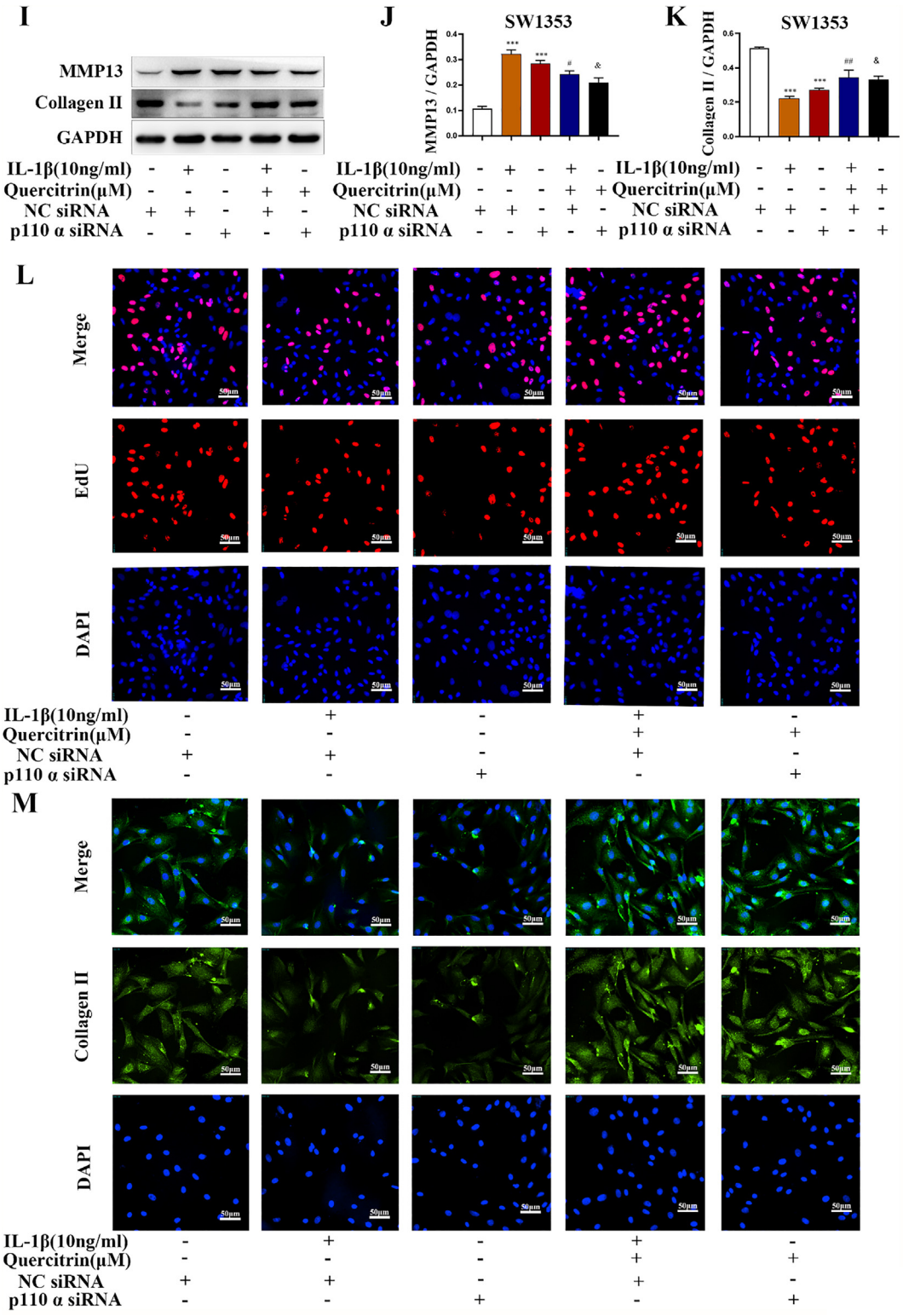

Fig. 3 (*continued*)

Specifically, cartilage from the 4 mg/kg quercitrin-treated group was less damaged and proteoglycans were increased relative to the low-dose group. The cartilage from the high-dose quercitrin-treated group was less damaged at 8 weeks and the proteoglycan levels were greater than at 4 weeks.

As shown in Fig. 4C-D, these results were also further confirmed by the OARSI scores, which are used to evaluate the severity of articular cartilage destruction. The OARSI scores results showed that the severity in ACLT rats at 8 weeks was much greater than at 4 weeks, which indicated that ACLT rats' joints become worse with time. At 4 and 8 weeks, the OARSI scores demonstrated that the 4 mg/kg quercitrin treatment group had markedly lower OARSI scores than the 2 mg/kg quercitrin treatment group after ACLT surgery compared with the ACLT rats. Furthermore, the OARSI scores

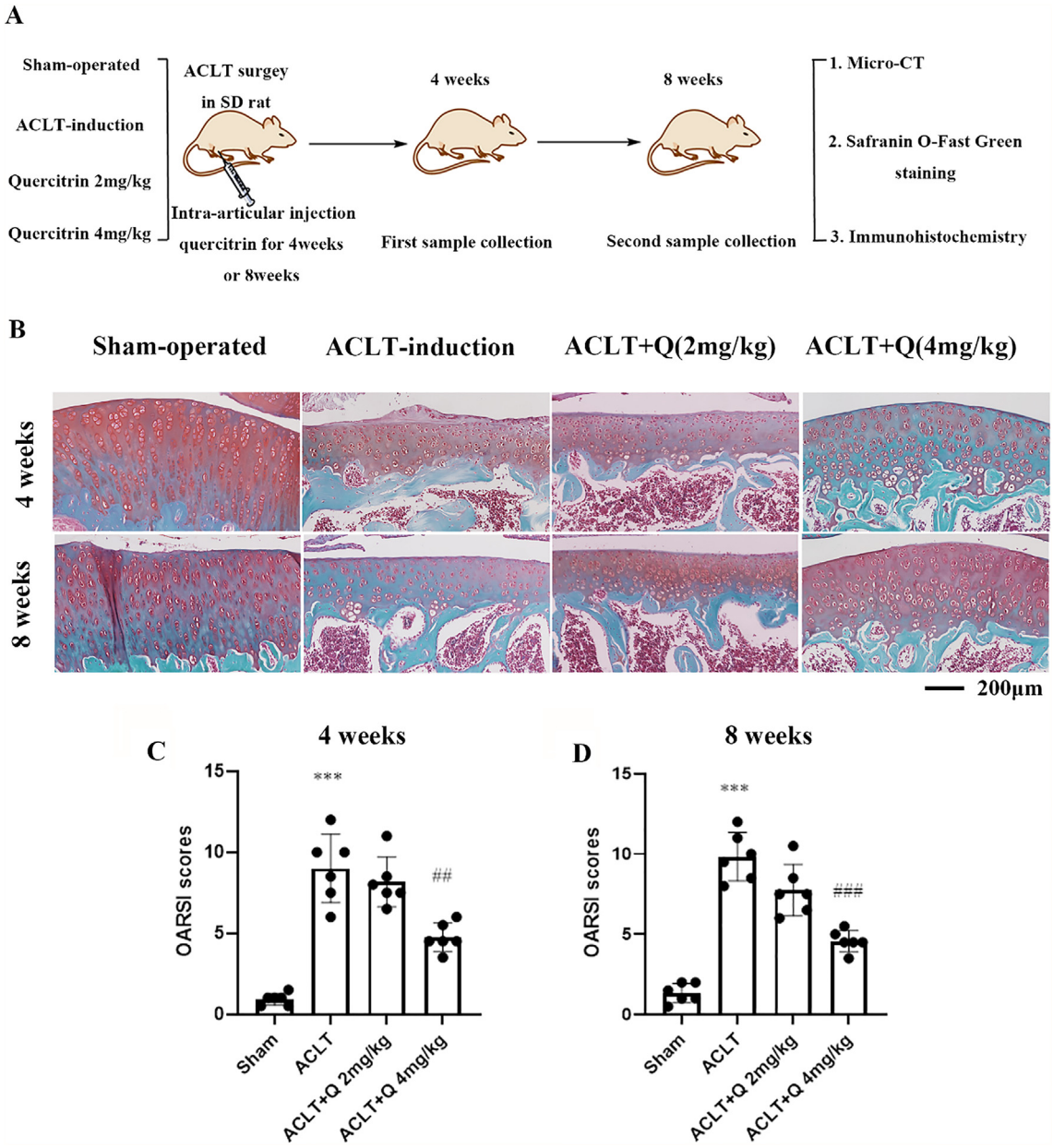

Fig. 4. Quercitrin attenuated cartilage degradation in ACLT rats. (A) Animal flow chart of quercitrin against OA. (B) Safranin O-Fast Green Staining of knee samples was performed at 4 and 8 weeks after ACLT surgery. (C–D) OARSI scores of articular cartilage at 4 and 8 weeks after ACLT surgery. All data are represented as mean ± SD. ***P < 0.001 versus the sham-operated group. ##P < 0.01 versus the ACLT-induction group. Data from OARSI scores were analyzed by using one-way ANOVA, followed by Tukey's range test (n = 6 for each group). (For interpretation of the references to colour in this figure legend, the reader is referred to the web version of this article.)

of the 4 mg/kg quercitrin treatment group were decreased at 8 weeks compared with the scores at 4 weeks.

Micro-CT analysis of quercitrin effects on tibial subchondral bone

To explore the effects of quercitrin on the tibia subchondral bone of ACLT rats at 4 and 8 weeks, the rat right tibial bones of rat were used for micro-CT scanning and 3D reconstruction. As revealed in Fig. 5A and B, the tibial subchondral bone showed significant changes between the sham-operated and ACLT-induction groups at 4 and 8 weeks. At 4 and 8 weeks, we observed that 4 mg/kg quercitrin treatment markedly alleviated all destruction of the tibial subchondral bone (Fig. 5B).

The values of BV/TV are shown in Fig. 5C and D. The average value of BV/TV in ACLT-induction group was 0.25 ± 0.03, which was lower than sham-operated group (0.34 ± 0.02) (P < 0.001) at 4 weeks (Fig. 5C). The average value of BV/TV was 0.32 ± 0.04 in ACLT-induction group, which was lower than sham-operated group (0.42 ± 0.01) (P < 0.001) at 8 weeks (Fig. 5D). Markedly differences were observed in the BV/TV of the tibial subchondral bone between the sham-operated and ACLT-induction rats, which displayed uncoupled bone remodeling in the tibial subchondral bone and increased bone resorption, resulting in bone loss in the ACLT-induction rats.

The average value of BV/TV was 0.30 ± 0.02 in 4 mg/kg quercitrin treatment group, which was higher than ACLT-induction group (0.25 ± 0.03) (P < 0.01) at 4 weeks (Fig. 5C). The average value of BV/TV was 0.41 ± 0.04 in 4 mg/kg quercitrin treatment group, which was higher than ACLT-induction group (0.32 ± 0.04) (P < 0.01) at 8 weeks (Fig. 5D). At 4 and 8 weeks, we observed that 4 mg/kg quercitrin treatment prominently alleviated tibial subchondral bone loss relative to the ACLT-induction rats.

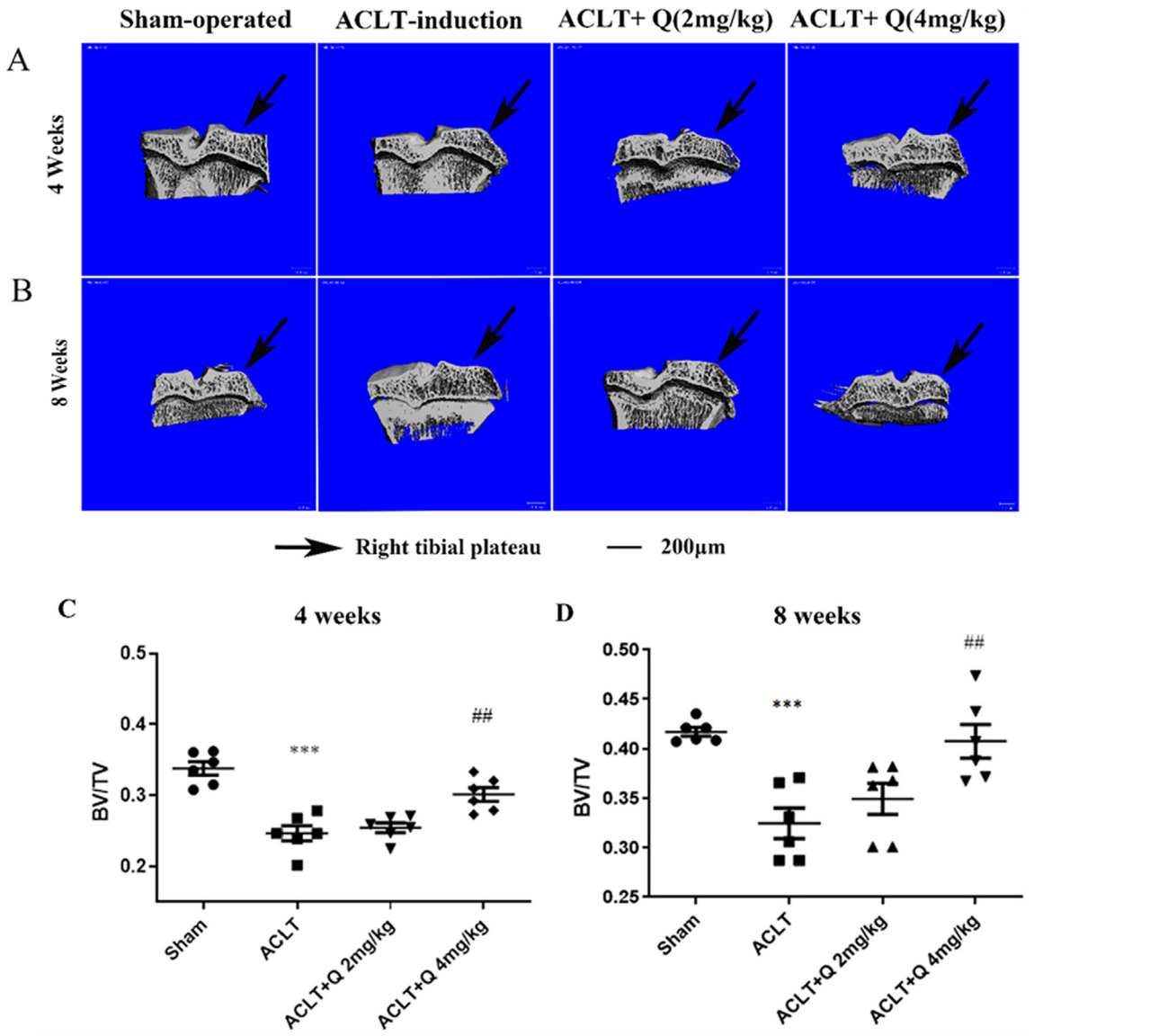

Fig. 5. Micro-CT analysis of quercitrin effects on the tibia after DMM surgery. (A) Micro-CT 3D reconstructions of tibial subchondral bones in ACLT rat knee joints were performed at 4 weeks after ACLT surgery. (B) Micro-CT 3D reconstructions of tibial subchondral bones in ACLT rat knee joints were performed at 8 weeks after ACLT surgery. (C-D) BV/TV were measured in the subchondral bone of rats at 4 and 8 weeks after ACLT surgery (n = 6 per group). All data are represented as the mean ± SD. ***P < 0.001, versus the sham-operated group. ##P < 0.01 versus the ACLT-induction group. Data from BV/TV were analyzed by using one-way ANOVA, followed by Tukey's range test.

Intra-articular injections of quercitrin in ACLT rats attenuates ECM degradation

Immunohistochemistry experiments of knee joint samples were performed to further investigate whether quercitrin attenuates OA progression by delaying ECM degradation in vitro. The results revealed that MMP13 protein expression in ACLT-induction group was significantly increased compared with sham group, and the treatment of quercitrin (2 mg/kg and 4 mg/kg) in ACLT rats for 4 and 8 weeks inhibited MMP13 protein expression (Fig. 6A). The results revealed that collagen Ⅱ protein expression in ACLT-induction group was significantly decreased compared with sham group, but was elevated in the ACLT rats treated with quercitrin (2 mg/kg and 4 mg/kg) for 4 and 8 weeks (Fig. 6B). These results also showed that the anti-OA effect of 4 mg/kg quercitrin treatment was better than 2 mg/kg quercitrin at 4 and 8 weeks. These results confirmed that intra-articular injection of 4 mg/kg quercitrin markedly delayed OA progression by delaying ECM

Fig. 6. Intra-articular injections of quercitrin in ACLT rats attenuate ECM degradation. (A) Paraffin wax sections were used to detect MMP13 expression with immunohistochemistry at 4 and 8 weeks after ACLT surgery. Solid arrows indicate positive staining for MMP13. (B) Paraffin wax sections were used to detect collagen II expression with immunohistochemistry at 4 and 8 weeks after ACLT surgery. Dotted arrows indicate positive staining for collagen II. (C) Paraffin wax sections were used to detect p110α expression with immunohistochemistry at 4 and 8 weeks after ACLT surgery. Circle indicate positive staining for p110α. (D) Quantitative analysis of the immunohistochemical staining of MMP 13 at 4 weeks. (E) Quantitative analysis of the immunohistochemical staining of MMP 13 at 8 weeks. (F) Quantitative analysis of the immunohistochemical staining of collagen Ⅱ at 4 weeks. (G) Quantitative analysis of the immunohistochemical staining of collagen Ⅱ at 8 weeks. (H) Quantitative analysis of the immunohistochemical staining of p110 α at 4 weeks. (I) Quantitative analysis of the immunohistochemical staining of p110 α at 8 weeks. All data are represented as the mean ± SD. *P < 0.05, **P < 0.01, ***P < 0.001 and versus sham-operated. #P < 0.05, ##P < 0.01 and ###P < 0.001 versus ACLT-induction. Data from immunohistochemistry experiments were analyzed by using one-way ANOVA, followed by Tukey's range test.

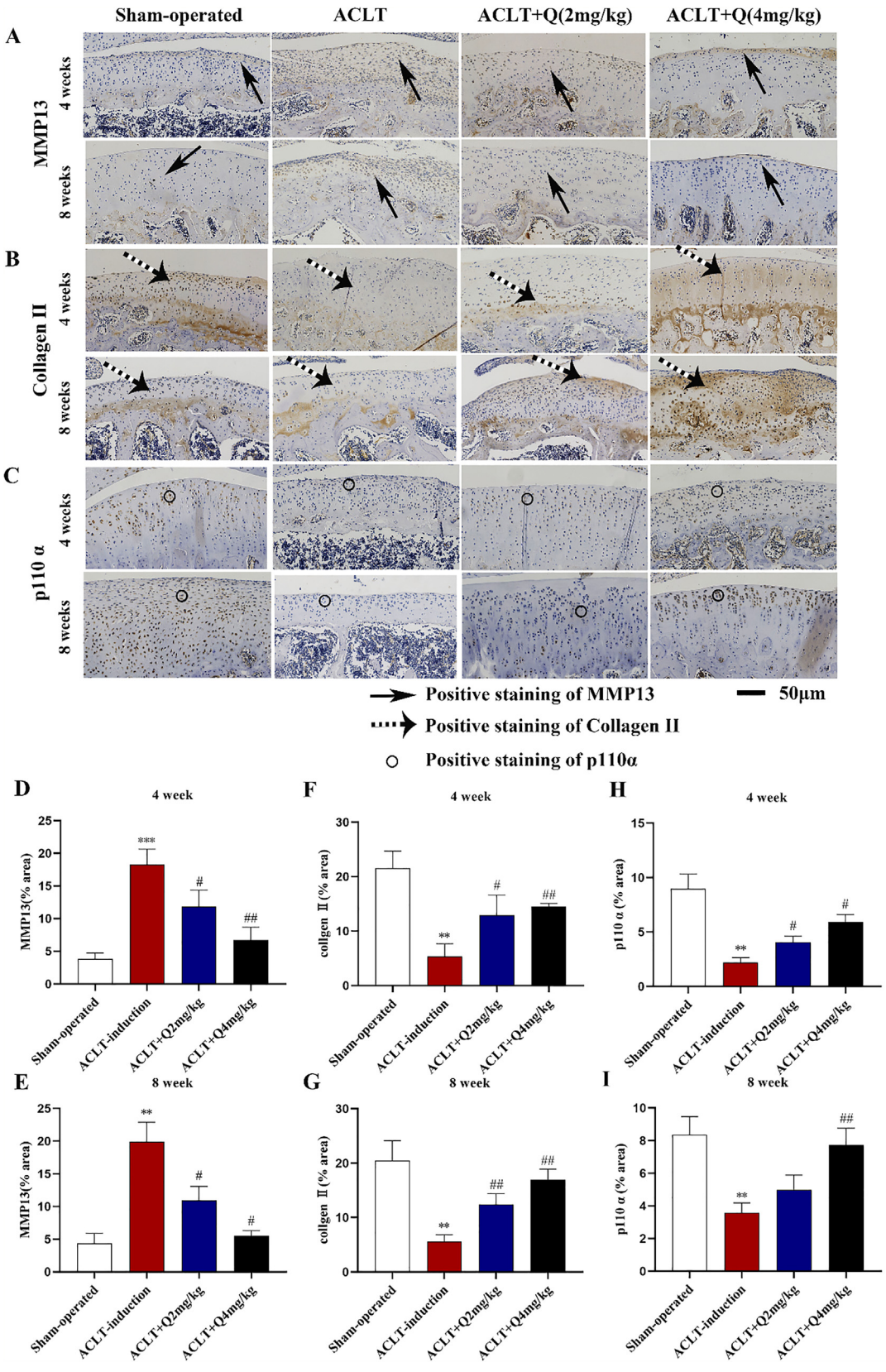
Sham-operated
ACLT
ACLT+Q(2mg/kg)
ACLT+Q(4mg/kg)
A
MMP13
4 weeks
8 weeks
B
Collagen II
4 weeks
8 weeks
C
p110 α
4 weeks
8 weeks
Positive staining of MMP13
50μm
Positive staining of Collagen II
Positive staining of p110α
D
4 week
MMP13(% area)
E
8 week
MMP13(% area)
F
4 week
collgen Ⅱ(% area)
G
8 week
collgen Ⅱ(% area)
H
4 week
p110 α (% area)
I
8 week
p110 α (% area)
Sham-operated
ACLT-induction
ACLT+Q2mg/kg
ACLT+Q4mg/kg

degradation in ACLT rats. Quantitative analysis of the immunohistochemical staining of MMP 13, collagen Ⅱ and p110α at 4 and 8 weeks was shown in Fig. 6D–G.

Furthermore, p110α expression levels decreased significantly in the OA-induction group relative to the sham-operated group (Fig. 6C), which is consistent with the results for articular cartilage in OA patients. Quantitative analysis of the immunohistochemical staining of p110α at 4 and 8 weeks was shown in Fig. 6H and I. At 4 and 8 weeks, 4 mg/kg quercitrin treatment significantly increased p110α protein expression.

Discussion

As we know, OA has long been considered a degenerative joint disease, as it has high prevalence and is an economical burden [1–4]. Disruptions in ECM degradation homeostasis play a significant role in the pathogenesis of OA [4,61,62], and MMP13 has a crucial role in ECM degradation because it affects the degradation of many ECM components [16,17], such as collagen Ⅱ.

Overexpression of MMP13 is regulated by complicated signals in the PI3K/AKT/mTOR pathway [25,26]. Growing evidence suggests that PI3K activation is currently caused by mutations in the p110α subunit, also called *PIK3CA*, in many cancers [32]; moreover, p110α is a significant drug target for cancer chemotherapy [33]. Increasing evidence suggests that PI3K is closely related to OA.

In this paper, our study first demonstrated that p110α mRNA expression levels were remarkably decreased in human OA cartilage compared with normal controls, which indicated p110α decreased is a prospective contributor to OA development, suggesting that p110α is a potential and crucial target for DMOAD development.

We are the first to report that quercitrin, a naturally occurring flavonoid, exerts anti-OA effects in vivo and in vitro. Quercitrin can promote cell proliferation and delay ECM degradation, including inhibiting MMP13 expression and increasing collagen Ⅱ accumulation by activating the p110α/AKT/mTOR signaling pathway in rat chondrocytes and SW1353 cells. We also analyzed the effects of *PIK3CA* silencing on EdU staining experiments and the expression of matrix biomarkers, including MMP13 and collagen Ⅱ, which suggested that quercitrin targets p110α to exert its anti-OA effects.

In further in vitro experiments, an ACLT rat model was used to assess the anti-OA effect of quercitrin. We suggested that intra-articular injection of quercitrin increased the BV/TV of tibial subchondral bone and cartilage thickness and reduced OARSI scores. We also proved that quercitrin exerts anti-OA effects by delaying ECM degradation, including inhibiting MMP13 expression and increasing collagen Ⅱ deposition.

The ACLT rat model simulates a traumatic form of OA and is reasonable to mimic of the pathogenesis of human OA. In this paper, the use of the ACLT rat model was somewhat limited because severe cartilage destruction occurs in the joints at 4 weeks after surgery. This is a universal limitation of all OA animal models [57]. Quercitrin was given 3 days after surgery and may work before OA begins. Therefore, our results indicated that quercitrin can slow down or prevent the onset of OA after injury. However, to date, we do not know why p110α mRNA levels are reduced in the articular cartilage of OA patients or how quercitrin works in combination with p110α. We will continue to study these questions in subsequent experiments.

Conclusions

In vitro, the results showed that p110α is a new target for OA therapeutic development. We demonstrated that quercitrin activated the p110α/AKT/mTOR signaling pathway by targeting p110α, revealing its promising potential in delaying the OA process by inhibiting cartilage ECM degradation and increasing chondrocyte proliferation. To further confirm its feasibility as a DMOAD for the prevention and treatment of early stage OA, an ACLT rat model was established to simulate OA in vivo. Intra-articular injections of quercitrin increased BV/TV of tibial subchondral bone and cartilage thickness and reduced the OARSI scores in OA rats. Meanwhile, we also suggested that quercitrin exerts anti-OA effect by inhibiting MMP13 expression and increasing collagen Ⅱ deposition in vivo. Our study indicated that quercitrin may be a promising DMOAD worth further investigation.

Declaration of Competing Interest

The authors declare that they have no known competing financial interests or personal relationships that could have appeared to influence the work reported in this paper.

Acknowledgments

This study was supported by the National Natural Science Foundation of China (No. 81673554) and the Postgraduate Research & Practice Innovation Program of Jiangsu Province (No. SJCX19_0161).

Appendix A. Supplementary material

Supplementary data to this article can be found online at https://doi.org/10.1016/j.jare.2020.06.020.

References

[1] Karsdal MA, Michaelis M, Ladel C, Siebuhr AS, Bihlet AR, Andersen JR, et al. Disease-modifying treatments for osteoarthritis (Dmoads) of the knee and hip: lessons learned from failures and opportunities for the future. Osteoarthritis Cartilage 2016;24(12):2013–21.
[2] Lotz MK, Carames B. Autophagy and cartilage homeostasis mechanisms in joint health, aging and Oa. Nat Rev Rheumatol 2011;7(10):579–87.
[3] Hunter DJ. Pharmacologic therapy for osteoarthritis–the era of disease modification. Nat Rev Rheumatol 2011;7(1):13–22.
[4] Vos T, Flaxman AD, Naghavi M, Lozano R, Michaud C, Ezzati M, et al. Years lived with disability (Ylds) for 1160 Sequelae of 289 diseases and injuries 1990–2010: a systematic analysis for the global burden of disease study 2010. The Lancet 2012;380:2163–96.
[5] Glyn-Jones S, Palmer AJR, Agricola R, Price AJ, Vincent TL, Weinans H, et al. Osteoarthritis. The Lancet 2015;386(9991):376–87.
[6] Yao X, Zhang J, Jing X, Ye Y, Guo J, Sun K, et al. Fibroblast growth factor 18 exerts anti-osteoarthritic effects through Pi3k-Akt signaling and mitochondrial fusion and fission. Pharmacol Res 2019;139:314–24.
[7] Dubois-Ferriere V, Lubbeke A, Chowdhary A, Stern R, Dominguez D, Assal M. Clinical outcomes and development of symptomatic osteoarthritis 2 to 24 years after surgical treatment of tarsometatarsal joint complex injuries. J Bone Joint Surg 2016;98(9):713–20.
[8] Kluzek S, Sanchez-Santos MT, Leyland KM, Judge A, Newton J, Arden NK. Painful knee but not hand osteoarthritis is an independent predictor of mortality over 23 years follow-up of a population-based cohort of middle-aged women. Ann Rheum Dis 2016;75(4):23.
[9] McGrory B, Jevsevar D, Weber K, Shea KG, Lynott JA, Bozic KJ, et al. The American academy of orthopaedic surgeons evidence-based clinical practice guideline on surgical management of osteoarthritis of the knee. J Bone Joint Surg Am 2016;98(8):688.
[10] Shi Y, Hu X, Cheng J, Zhang X, Zhao F, Shi W, et al. A small molecule promotes cartilage extracellular matrix generation and inhibits osteoarthritis development. Nat Commun 2019;10(1):1914.
[11] van der Kraan PM, van den Berg WB. Chondrocyte hypertrophy and osteoarthritis: role in initiation and progression of cartilage degeneration?. Osteoarthritis Cartilage 2012;20(3):223–32.
[12] Goldring MB. Update on the biology of the chondrocyte and new approaches to treating cartilage diseases. Best Pract Res Clin Rheumatol 2006;20(5):1003–25.
[13] Huang K, Wu L. Aggrecanase and aggrecan degradation in osteoarthritis: a review. J Int Med Res 2008;36:1149–60.
[14] Poole AR, Kobayashi M, Yasuda T, Laverty S, Mwale F, Kojima T, et al. Type II collagen degradation and its regulation in articular cartilage in osteoarthritis. Ann Rheum Dis 2002;61:78–81.

[15] Sandell LJ, Aigner T. Articular cartilage and changes in arthritis an introduction: cell biology of osteoarthritis. J Arthritis 2001;3:107–13.
[16] Goldring MB, Marcu KB. Cartilage homeostasis in health and rheumatic diseases. Arthritis Res Ther 2009;11(3):224.
[17] Fosang AJ, Last K, Knauper V, Murphy G, Neame PJ. Degradation of cartilage aggrecan by collagenase-3 (Mmp-13). FEBS Lett 1996;380:17–20.
[18] Wang M, Sampson ER, Jin H, Li J, Ke QH, Im H-J, et al. Mmp13 is a critical target gene during the progression of osteoarthritis. Arthritis Res Ther 2013;15:5.
[19] Mitchell PG, Magna HA, Reeves LM, Lopresti-Morrow LL, Yocum SA, Rosner PJ, et al. Cloning, expression, and type II collagenolytic activity of matrix metalloproteinase-13 from human osteoarthritic cartilage. J Clin Invest 1996;97:761–8.
[20] Kim JH, Jeon J, Shin M, Won Y, Lee M, Kwak JS, et al. Regulation of the catabolic cascade in osteoarthritis by the Zinc-Zip8-Mtf1 axis. Cell 2014;156(4):730–43.
[21] Corciulo C, Lendhey M, Wilder T, Schoen H, Cornelissen AS, Chang G, et al. Endogenous adenosine maintains cartilage homeostasis and exogenous adenosine inhibits osteoarthritis progression. Nat Commun 2017;8:15019.
[22] Jeon OH, Kim C, Laberge R-M, Demaria M, Rathod S, Vasserot AP, et al. Local clearance of senescent cells attenuates the development of post-traumatic osteoarthritis and creates a pro-regenerative environment. Nat Med 2016;23:775–82.
[23] Zhang M, Lygrisse K, Wang J. Role of microrna in osteoarthritis. J Arthritis 2017;6(2):1–12.
[24] Si HB, Zeng Y, Liu SY, Zhou ZK, Chen YN, Cheng JQ, et al. Intra-articular injection of Microrna-140 (Mirna-140) alleviates osteoarthritis (Oa) progression by modulating extracellular matrix (Ecm) homeostasis in rats. Osteoarthritis Cartilage 2017;25(10):1698–707.
[25] Cai C, Min S, Yan B, Liu W, Yang X, Li L, et al. Mir-27a promotes the autophagy and apoptosis of Il-1β treatedarticular chondrocytes in osteoarthritis through Pi3k_Akt_Mtor signaling. Aging 2019;11:6371–84.
[26] Engelman JA. Targeting Pi3k signalling in cancer: opportunities challenges and limitations. Nat Rev Cancer 2009;9(8):550–62.
[27] Yu M, Gu Q, Xu J. Discovering new Pi3kalpha inhibitors with a strategy of combining ligand-based and structure-based virtual screening. J Comput Aided Mol Des 2018;32(2):347–61.
[28] Lien EC, Dibble CC, Toker A. Pi3k signaling in cancer: beyond Akt. Curr Opin Cell Biol 2017;45:62–71.
[29] Denley A, Kang S, Karst U, Vogt P. Oncogenic signaling of class I Pi3k isoforms. Oncogene 2008;27:2561–74.
[30] Yap TA, Garrett MD, Walton MI, Raynaud F, Bono JSD, Workman P. Targeting the Pi3k-Akt-Mtor pathway_ progress, pitfalls, and promises. Curr Opin Pharmacol 2008;8(4):394–412.
[31] Janku F, Tsimberidou AM, Garrido-Laguna I, Wang X, Luthra R, Hong DS, et al. Pik3ca mutations in patients with advanced cancers treated with Pi3k/Akt/Mtor axis inhibitors. Mol Cancer Ther 2011;10(3):558–65.
[32] Ligresti G, Militello L, Steelman LS, Cavallaro A, Basile F, Nicoletti F, et al. Pik3ca mutations in human solid tumors: role in sensitivity to various therapeutic approaches. Cell Cycle 2009;8(9):1352–8.
[33] Lu J, Ji ML, Zhang XJ, Shi PL, Wu H, Wang C, et al. Microrna-218-5p as a potential target for the treatment of human osteoarthritis. Mol Ther 2017;25(12):2676–88.
[34] Cravero JD, Carlson CS, Im H-J, Yammani RR, Long D, Loeser RF. Increased expression of the Akt_Pkb inhibitor Trb3 in osteoarthritic chondrocytes inhibits insulin-like growth factor 1–mediated cell survival and proteoglycan synthesis. Arthrit Rheum-Arthr 2009;60:492–500.
[35] Zhang Y, Vasheghani F, Li Y, Blati M, Kayla S, Fahmi H, et al. Cartilage-specific deletion of Mtor upregulates autophagy and protects mice from osteoarthritis. Osteoarthr Cartilage 2014;22:340.
[36] Cui X, Wang S, Cai H, Lin Y, Zheng X, Zhang B, et al. Overexpression of Microrna-634 suppresses survival and matrix synthesis of human osteoarthritis chondrocytes by targeting Pik3r1. Sci Rep 2016;6:23117.
[37] Liu XL, Zhao L, Xu ND, He FJ. Treatment of Chinese medicine in early, mid-term period of knee osteoarthritis. J Changchun Univ Traditional Chin Med 2014;5(30):918–9.
[38] Huang PT. Data mining and clinical drug efficacy analysis on Chinese medicine treatment of knee osteoarthritis [dissertation]. Jiangsu (China): Nanjing University of Chinese Medicine; 2015.
[39] Liu CY, Chiu YJ, Wu LY, Chao LK, Peng WH. Analgesic and anti-inflammatory activities of the ethanol extract of Taxillus sutchuenensis in mice. Afr J Pharm Pharmacol 2013;7(23):1546–53.
[40] Fabjan N, Rode J, Kosir IJ, Wang Z, Zhang Z, Kreft I. Tartary Buckwheat (Fagopyrum Tataricum Gaertn.) as a Source of Dietary Rutin and Quercitrin. J Agr Food Chem 2003;51(22):6452–5.
[41] B. AW, H. GR, B. A. Health effects of quercitrin: from antioxidant to nutraceutical. Eur J Pharmacol 2008;585(2–3):325–37.
[42] Zhang M, Swarts S, Yin L, Liu C, Tian Y, Cao Y, et al. Antioxidant properties of quercitrin. Adv Exp Med Biol 2011;701:283–9.
[43] A.P. Rogerio, A. Kanashiro, C. Fontanari, E.V.G.D. Silva, Y.M. Lucisano-Valim, E. G. Soares, L.H. Faccioli. Anti-inflammatory activity of quercetin and isoquercitrin in experimental murine allergic asthma. INFLAMM RES 2007;56:402–8.
[44] B. AW, W. LC, S. EL, K. JC, B. A, H. GR. In vitro and ex vivo anti-inflammatory activity of quercitrin in healthy volunteers. Nutrition 2008;24(7–8):703–10.
[45] L. BH, J. SM, L. JH, K. JH, Y. IS, L. JH, C. SH, L. SM, C. CG, K. HC, H. Y, P. HD, K. Y, N. SY. Quercitrin inhibits the 5-hydroxytryptamine type 3 receptor-mediated ion current by interacting with pre-transmembr quercitrin domain I. Mol Cells 2005;20(1):69–73.
[46] Satue M, Arriero Mdel M, Monjo M, Ramis JM. Quercitrin and taxifolin stimulate osteoblast differentiation in Mc3t3-E1 cells and inhibit osteoclastogenesis in raw 264.7 cells. Biochem Pharmacol 2013;86(10):1476–86.
[47] Choi EM. Protective effect of quercitrin against hydrogen peroxide-induced dysfunction in osteoblastic Mc3t3-E1 cells. Exp Toxicol Pathol 2012;64(3):211–6.
[48] Xing LZ, Ni HJ, Wang YL. Quercitrin attenuates osteoporosis in ovariectomized rats by regulating mitogen-activated protein kinase (Mapk) signaling pathways. Biomed Pharmacother 2017;89:1136–41.
[49] Jiang L, Li L, Geng C, Gong D, Jiang L, Ishikawa N, et al. Monosodium iodoacetate induces apoptosis via the mitochondrial pathway involving ros production and caspase activation in rat chondrocytes in vitro. Inc J Orthop Res 2013;31:364–9.
[50] Lu W, Shi J, Zhang J, Lv Z, Guo F, Huang H, et al. Cxcl12_Cxcr4 axis regulates aggrecanase activation and cartilage degradation in a post-traumatic osteoarthritis rat model. Int J Mol Sci 2016;17:1522.
[51] Kang L, Yang C, Song Y, Liu W, Wang K, Li S, et al. Microrna-23a-3p promotes the development of osteoarthritis by directly targeting Smad3 in chondrocytes. Biochem Bioph Res Co 2016;478:467–73.
[52] Guo J, Li W, Wu Y, Jing X, Huang J, Zhang J, et al. Meclizine prevents ovariectomy-induced bone loss and inhibits osteoclastogenesis partially by upregulating Pxr. Front Pharmacol 2017;8:693.
[53] Hu Y, Gui Z, Zhou Y, Xia L, Lin K, Xu Y. Quercetin alleviates rat osteoarthritis by inhibiting inflammation and apoptosis of chondrocytes, modulating synovial macrophages polarization to M2 macrophages. Free Radic Biol Med 2019;145:146–60.
[54] Zhou X, Xia Y, Zhang Y, Luo J, Han C, Zhang H, et al. Tomentodione M Sensitizes multidrug resistant cancer cells by decreasing P-glycoprotein via inhibition of P38 Mapk signalling (article). Oncotarget 2017;8:101965–83.
[55] Jian K, Zhang C, Shang Z, Yang L, Kong L-Y. Eucalrobusone C Suppresses cell proliferation and induces Ros-dependent mitochondrial apoptosis via the P38 Mapk pathway in hepatocellular carcinoma cells. Phytomedicine 2017;25:71–82.
[56] Luo J, Xia Y, Luo J, Junhe Li C, Zhang H, Zhang T, et al. Grp78 inhibition enhances Atf4-induced cell death by the deubiquitination and stabilization of chop in human osteosarcoma. Cancer Lett 2017;410:112–23.
[57] Weng T, Xie Y, Yi L, Huang J, Luo F, Du X, et al. Loss of Vhl in cartilage accelerated the progression of ageassociated and surgically induced murine osteoarthritis. NIH Public Access 2014;22(8):1197–205.
[58] Dong Y, Liu H, Zhang X, Xu F, Qin L, Cheng P, et al. Inhibition of Sdf-1alpha/Cxcr4 signalling in subchondral bone attenuates post-traumatic osteoarthritis. Int J Mol Sci 2016;17(6).
[59] Gerwin N, Bendele AM, Glasson S, Carlson CS. The Oarsi histopathology initiative – recommendations for histological assessments of osteoarthritis in the rat. Osteoarthritis Cartilage 2010;18(Suppl 3):24–34.
[60] Wang Z, Huang J, Zhou S, Luo F, Xu W, Wang Q, et al. Anemonin attenuates osteoarthritis progression through inhibiting the activation of Il-1beta/Nf-Kappab pathway. J Cell Mol Med 2017;21(12):3231–43.
[61] Yan S, Wang M, Zhao J, Zhang H, Zhou C, Jin L, et al. Microrna-34a affects chondrocyte apoptosis and proliferation by targeting the Sirt1/P53 Signaling pathway during the pathogenesis of osteoarthritis. Int J Mol Med 2016;38(1):201–9.
[62] Xia B, Di C, Zhang J, Hu S, Jin H, Tong P. Osteoarthritis pathogenesis: a review of molecular mechanisms. Calcif Tissue Int 2014;95(6):495–505.